

## Mixing in curved tubes

Vimal Kumar\*, Mohit Aggarwal, K.D.P. Nigam

*Department of Chemical Engineering, Indian Institute of Technology Delhi, Hauz Khas, New Delhi-110016, India*

Received 29 December 2005; received in revised form 19 April 2006; accepted 29 April 2006

Available online 9 May 2006

### Abstract

The mixing efficiency in a curved tube is a complex function of the Reynolds number, Schmidt number, curvature ratio and tube pitch, therefore, the relative effectiveness of a helical tube is quite complicated and challenging over a straight tube. A state of art review on mixing of two miscible liquids in curved tubes revealed that the mixing in coils of circular cross section has not been reported in the literature. In the present work a computational fluid dynamics study is performed in curved tubes of circular cross-section of finite pitch under laminar flow conditions to examine the scalar mixing of two miscible fluids using scalar transport technique. In the present study the phenomenon of mixing by convection and diffusion of two flow streams with inlet scalar concentrations of zero and unity in the two halves of a tube perpendicular to the plane of curvature has been reported. The mixing efficiency has been quantified with concentration distributions and unmixedness coefficient at different cross-sections and process conditions (Reynolds number, Schmidt number and curvature ratio) in the straight and curved tube of circular cross-section. The result shows that, in curved tube, for higher Schmidt number fluids, mixing is considerably improved at moderately low Reynolds numbers ( $Re \sim 10$ ), but is not affected for Reynolds number of the order of 0.1. It is also reported that mixing in the curved tube is higher at low values of curvature ratio as compared to the higher curvature ratio.

© 2006 Elsevier Ltd. All rights reserved.

*Keywords:* Scalar mixing; Straight tube; Helical tube; Computational fluid dynamics

### 1. Introduction

Mixing is an essential component of nearly all industrial chemical processes, ranging from simple blending to complex multi phase reaction systems for which reaction rate, yield and selectivity are highly dependent upon mixing performance. Consequences of improper mixing include non-reproducible processing conditions and lowered product quality, resulting in the need for more elaborate downstream purification processes and increased waste disposal costs. Despite its importance, however, mixing performance is seldom characterized rigorously for industrial systems. Detailed characterization are important, particularly in slow-moving laminar flows of high viscosity materials which have a serious potential to lead to inhomogeneity and poorly mixed regions within the flow systems. The fluids to be mixed are usually liquid with small diffusion coefficients. Mixing of liquid solutions in the micro-channels is

slow partly due to the low diffusivity of molecules in liquids. A pipe of a length of 100–200 diameters would be needed to get a well-mixed fluid, which seems to be impracticable. For the mixers that have the dimensions of the order of tens of microns, the molecular diffusion based mixing time is of the order of seconds, while mixers with dimension of the order of hundreds of microns, molecular diffusion based time for complete mixing can be of the order of tens of seconds. Therefore diffusion times are large. Recently with the advent of new innovative devices, many studies have been performed aiming at providing an efficient method of mixing under laminar conditions.

In the literature, the numerous mixer designs have been proposed, and are classified into two main categories: active and passive. In active mixing, the energy input for mixing is derived from the external source, while in case of passive mixing flow energy is utilized to restructure the flow in a way that results in improved mixing (due to pumping action or hydrostatic potential). Active mixer produces excellent mixing, but they are often difficult to fabricate and maintain. Passive mixers are attractive because of their ease of operation and manufacture. Table 1 shows some of the active and passive mixing techniques.

\* Corresponding author. Tel./fax: +91 11 26591020.  
drkdpn@gmail.com (K.D.P. Nigam).

Table 1  
Characterization of mixing processes at microscale

Approach	Reference
<i>A. Active mixing</i>	
Ultrasound	Yang et al. (2001)
Acoustic, bubble-induced vibration	Liu et al. (2002, 2003); Evans et al. (1997); Deshmukh et al. (2000)
Electrokinetic instabilities	Oddy et al. (2001)
Periodic vibration of flow rate	Glasgow and Aubry (2003) Niu and Lee (2003) Qian and Bau (2002) Volpert et al. (1999) Lee et al. (2001)
Electrowetting-induced merging of droplets	Palk et al. (2003)
Piezoelectric vibrating membranes	Woiias et al. (2000)
Magneto-hydrodynamic action	West et al. (2002)
Impellers	Lu et al. (2001)
Integrated microvalves/pumps	Voldman et al. (1998)
<i>B. Passive mixing</i>	
Interdigital multi-lamellae arrangement	Bessoth et al. (1999); Branebjerg et al. (1996); Drese (2003); Ehlers et al. (2000); Ehrfeld et al. (1999); Floyd et al. (2000); Hardt and Schönfeld (2003); Hessel et al. (2003); Löb et al. (2004); Zech et al. (2000)
Split-and-recombine concepts (SAR)	Branebjerg et al. (1996); Schönfeld et al. (2004); Schwesinger et al. (1996)
Chaotic mixing by eddy formation and folding	Saxena and Nigam (1984); Jen et al. (2003); Jiang et al. (2004); Lee et al. (2001); Liu et al. (2001); Niu and Lee (2003); Qian and Bau (2002); Solomon and Mezic (2003); Stroock et al. (2002a, b);
Nozzle injection in flow	Miyake et al. (1993);
Collision of jets	Penth (1999); Werner et al. (2002)
Coanda-effect	Hong et al. (2001)

In the present work curved tube of circular cross-section has been considered to characterize the mixing as it is extensively used in industrial practice. Dean (1927, 1928) was the first to investigate flow in helically coiled circular tubes, and found that a pair of symmetric vortices was formed on the cross sectional plane due to centrifugal force (Fig. 1). The strength of secondary flow is characterized by Dean number,

$$De = Re/\sqrt{\lambda}, \quad (1)$$

where  $\lambda$  is the curvature ratio and is defined as the ratio of coil radius to tube radius i.e.,  $\lambda = R_c/a$ . Extensive reviews on flow fields in curved ducts were reported by Berger et al. (1983), Shah and Joshi (1987) and Nandakumar and Masliyah (1986). These studies have been focused to discuss the effect of secondary flows; enhanced shear stress and heat transfer rates. However to the best of our knowledge, no previous study has been reported to study the mixing efficiency in the curved tube of circular cross-section.

Liu et al. (2000) and Yi and Bau (2000) used a series of short rectangular bends to produce the stirring of the two fluids. The bend-induced cross-stream vortices generated in their work were observed to decay quickly in the downstream straight sections of the bend tubes because of the viscous effects. Schönfeld and Hardt (2003) proposed a different concept of chaotic mixing which relies on helical flows induced in planar curved channels. In the micromixers proposed by them, the mixing time was in the range of milliseconds, thus lending towards the fast, mass-transfer-limited reactions. Jiang et al. (2004) and Vanka et al. (2004) studied in contrast to

the designs reported previously, only simple planar channel geometry without multi-step or three-dimensional (3-D) structures is sufficient to induce chaotic mixing. Vanka et al. (2004) have studied the mixing in square cross-sectional curved ducts while Jiang et al. (2004) have proposed a s-shaped geometry to generate chaotic flows by alternating switching between different flow patterns. However these studies have been performed for planar curved ducts with square cross section and zero pitch.

The number of investigations to the mixing mechanisms is limited, probably due to experimental difficulties. The recent advancements in Computational Fluid Dynamics (CFD) have raised the question to which extent computer simulations can be used as a tool in the design and analysis of helical mixers. In the area of characterizing mixer performance, CFD has been used in a number of cases (Byrde and Sawley, 1999; Fourcade et al., 2001; Bakker et al., 1998). A series of mixing criteria have been reported to assess the ability of a given mixer. Some of these criteria are based on chaos analysis, the level of chaos giving an indication on mixing efficiency. In the present work, mixing efficiency in helical tubes with non-zero pitch and circular cross section have been studied using the criterion of unmixedness coefficient as discussed by Vanka et al. (2004) for planar geometry. The mixing efficiency has been quantified with concentration distributions and unmixedness coefficient at different cross-section and at different process conditions (Reynolds number, Schmidt number and curvature ratio) in the straight and curved tube of circular cross-section.

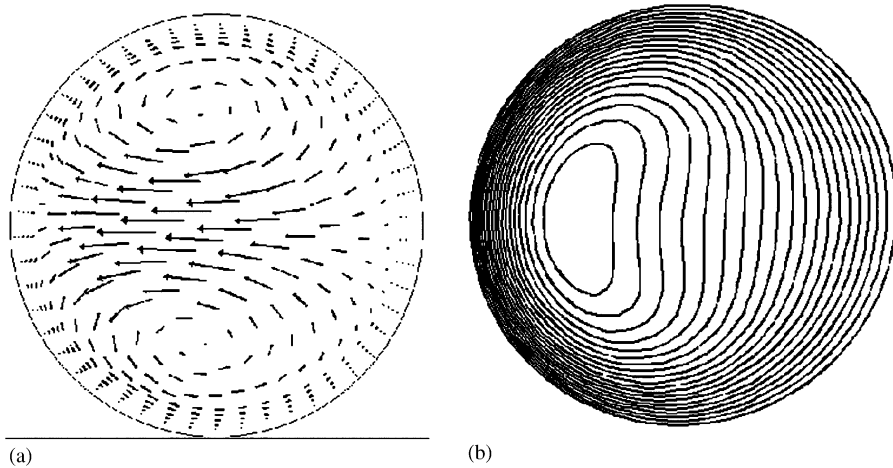


Fig. 1. Dean vortices (a) and axial velocity contours (b) in the curved tube of circular cross-section.

## 2. Numerical model

The geometry considered and the systems of coordinates used in the present study are shown in Fig. 2. The circular pipe has a diameter of  $2a$  and is coiled at a radius of  $R_c$ , while the distance between two turns (the pitch) is represented by  $H$ . The Cartesian coordinate system is used in numerical simulation to represent a helical pipe. Since it is assumed that the two liquids are miscible and have similar properties, the flow profiles were calculated with only a single fluid. Fully developed velocity profiles were employed at the inlet of the curved tube. The regime of greatest interest for mixing is for the small Reynolds number (0.1, 1, 5 and 10) where the inertia effects to be substantially absent. In this regime, the flow becomes largely independent of Reynolds number as the flow field in the mixing channel reaches its developed state within a distance less than approximately one tube diameter (Boussinesq, 1891); the hydrodynamic developing length in the straight tube is,  $L/d = 0.065 Re$  (Durst et al., 2005). The study was performed for Reynolds number varying from 0.1 to 100 with Schmidt number varying from 1 to 1000 and curvature ratio from 5 to 10. The simulations were carried out for a dimensionless finite pitch of 0.024 ( $H' = H/2\pi R_c$ ). The scalar transport technique was used to simulate the flow of two miscible liquids. Once the steady state solution was established, the transport equations of a scalar were solved over the fixed flow field to determine the mixing characteristics. The governing equations for three-dimensional laminar flow in the curved tube could be written in the master Cartesian coordinate system as

*Continuity equation:*

$$\frac{\partial u_i}{\partial x_i} = 0. \quad (2)$$

*Momentum equation:*

$$\frac{\partial}{\partial x_j} \left[ \mu \left( \frac{\partial u_i}{\partial x_j} + \frac{\partial u_j}{\partial x_i} \right) - \rho u_j u_i - \delta_{ij} p \right] = 0. \quad (3)$$

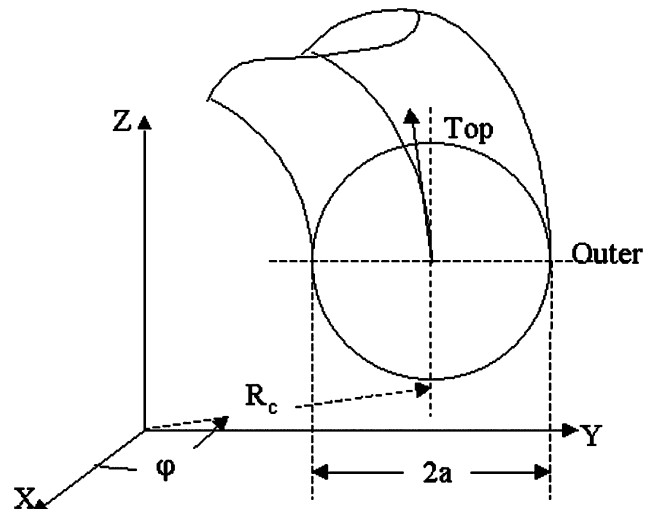


Fig. 2. Coordinate system used for the computation.

*Scalar transport:*

$$\frac{\partial}{\partial x_j} \left[ \Gamma \left( \frac{\partial c}{\partial x_j} \right) - \rho u_j c \right] = 0, \quad (4)$$

where  $\rho$  is the density of fluid,  $u$  is the velocity of fluid and  $\Gamma$  is the diffusion coefficient.

No-slip boundary condition, i.e.,  $u_i = 0$ , and the zero derivative conditions for the scalars were imposed on the wall. At the inlet of the curved duct, the scalar concentrations of 0 and 1 were prescribed in the two halves of the duct perpendicular to the plane of curvature. The scalar concentration was initialized such that the interface was perpendicular to the direction of the secondary flow. The flow fields were solved first because the values of density and viscosity did not influenced by the scalar fields. The convection term in the governing equations was modeled with the bounded second-order upwind scheme and the diffusion term was computed using the multilinear interpolating polynomials nodes  $N_i(X, Y, Z)$ . The SIMPLE algorithm is used to resolve

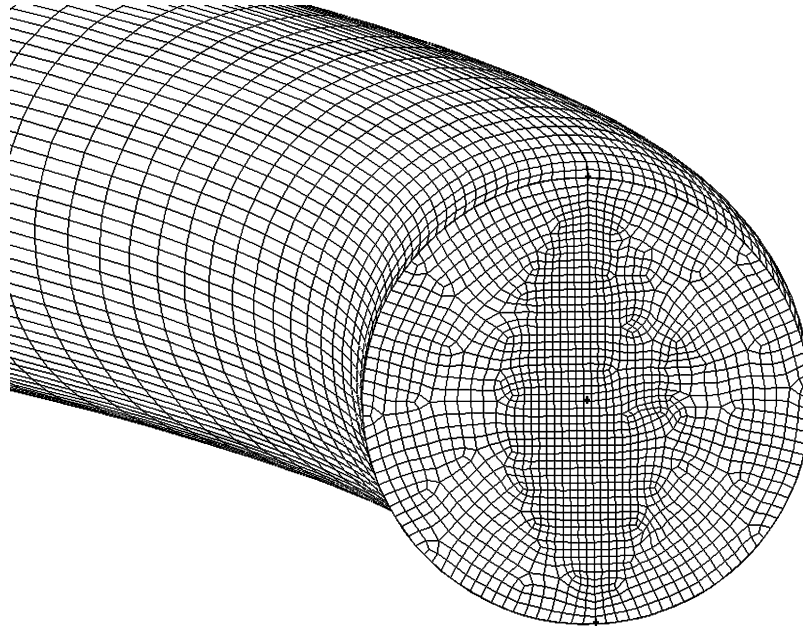


Fig. 3. Grid topology at a cross-section.

the coupling between velocity and pressure (Patankar et al., 1974).

The grid was generated with Gambit<sup>TM</sup> and exported to Fluent 6.2 for performing the flow and mixing computations. The computational domain considered in the present work is of coil with 4 turns. Unstructured grid was considered for the present study as shown in Fig. 3. Fully developed velocity profile was prescribed at the inlet. About 800 iterations were needed to achieve convergence of steady state solution. Starting the computation with a relatively accurate initial guess for the flow field had a positive effect on the speed of convergence. The numerical computation is considered converged when the residual summed over all the computational nodes at  $n$ th iteration,  $R_\phi^n$ , satisfies the following criterion:  $R_\phi^n / R_\phi^m \leq 10^{-8}$ , where  $R_\phi^m$  denotes the maximum residual value of  $\phi$  variable after  $m$  iterations,  $\phi$  applied for  $p$ ,  $u_i$ , and for scalars. After the flow field is fixed, the scalar transport needed only 10–15 iterations for convergence and the residuals for scalar attained similar levels as for flow calculations.

In order to quantify the mixing efficiency we used the unmixedness coefficient defined for a cross sectional area as,

$$\theta = \frac{\int [\bar{c} - c(x_i)]^2 dA}{\bar{c}}, \quad (5)$$

where  $\theta$  is the unmixedness coefficient. This represents the root mean square average deviation of the fluid from complete mixing. The quantity  $\bar{c}$  represents a local area weighted mean concentration over the cross-section given by

$$\bar{c} = \frac{1}{A} \int_0^A c(x_i) dA. \quad (6)$$

Thus higher the value of  $\theta$  lower is the mixing and for complete mixing  $\theta$  is zero.

### 2.1. Grid independence test

The grid independent test for both flow fields and scalar fields were reported separately. For flow fields the grid-sensitivity tests were carried out with four grids consisting of  $353 \times 200$ ,  $432 \times 300$ ,  $625 \times 200$  and  $1390 \times 200$  (cross-section  $\times$  axial mesh). Fig. 4a shows the velocity profiles in horizontal centerline at the outlet of the curved tube at  $Re = 100$  and  $\lambda = 10$  for all the grid systems. It can be seen from these plots that the  $625 \times 200$  grid gave good accuracy, given that the velocity profiles agreed closely with the solution on the  $1390 \times 200$  grids. The fully developed velocity profiles in the present work were also compared with the experimental and analytical data of Mori and Nakayama (1965) and numerical data of Patankar et al. (1974) to validate implementation of curvature and FLUENT predictions at higher Reynolds number. Fig. 5 shows that the present predictions using FLUENT are in good agreement with the predictions of Mori and Nakayama (1965) and Patankar et al. (1974). The flow pattern at intermediate Reynolds number were also compared and found in good agreement to those observed by the previous investigators (Jones et al., 1989; Duchene et al., 1995; Kumar and Nigam, 2005).

For the scalar field, grid independence was more difficult when the Schmidt number was high. As a result, much higher resolutions were needed for grid-independent mixing efficiencies. A systematic grid sensitivity investigation was performed at  $Sc = 1000$  and  $Re = 20$ , with grids as fine as  $3416 \times 400$  (cross-sectional  $\times$  axial grid) control volumes for a curved channel of curvature ratio  $\lambda$  of 5. Fig. 4b shows the

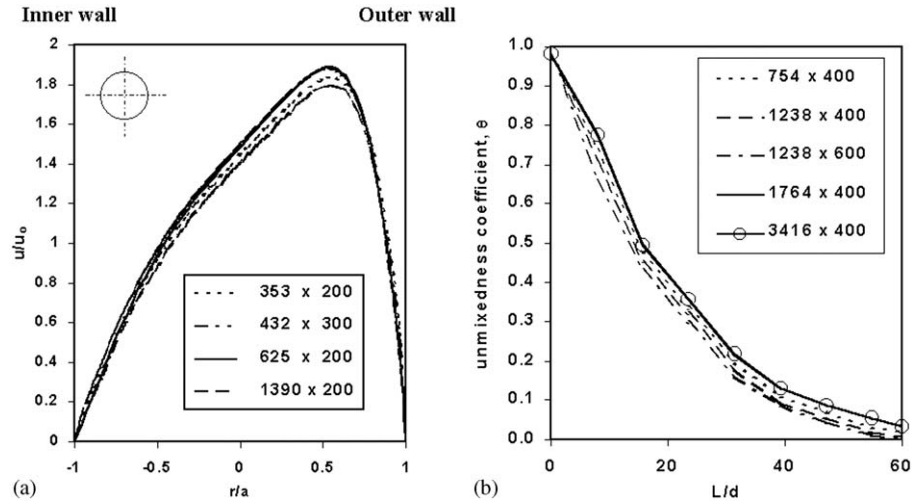


Fig. 4. Grid independent test: (a) velocity profiles in horizontal centerline at the outlet of the curved tube ( $Re = 100$  and  $\lambda = 10$ ); and (b) unmixedness coefficient as a function of distance along helical tube ( $\lambda = 5$ ) for different Grid sizes shown as, number of cells in a cross-section  $\times$  divisions/ $90^\circ$  turn.

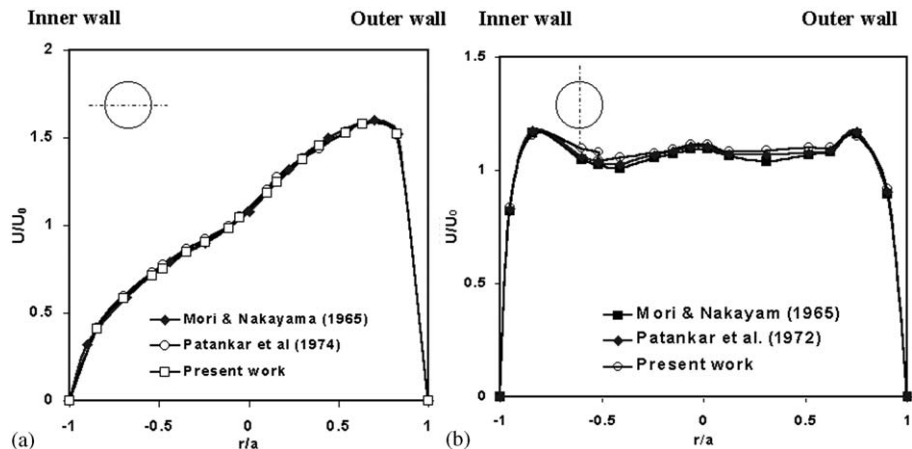


Fig. 5. Comparison of velocity profiles at  $De = 632.4$ ,  $D/d = 40$  with experimental data of Mori and Nakayama (1965) and computational data of Patankar et al. (1974) at: (a) horizontal centerline; and (b) vertical centerline.

unmixedness coefficient (defined by Eq. (5)) as a function of streamwise distance for different grids. It can be seen that a  $1764 \times 400$  grid was necessary to obtain grid-independent results at  $Sc = 1000$ .

### 3. Results and discussion

#### 3.1. Straight tube

In order to standardize the technique the computations were first carried out in straight tube geometry. The simulations were carried out on half cross-section of the tube to avoid the large number of cells in the straight tube geometry. Fig. 6 shows the scalar concentration profile for various planes in the straight tube cross-section for different values of  $Re Sc = 100$  (i.e.,  $Re = 100$  and  $Sc = 1$ ),  $Re Sc = 1000$  (i.e.,  $Re = 0.1$  and  $Sc = 1000$ ) and  $Re Sc = 20,000$  (i.e.,  $Re = 20$  and  $Sc = 1000$ ). The fully

developed non-dimensional velocity profiles were independent of the Reynolds number; therefore, the concentration profile is a function of Peclet number (i.e., the product of the Reynolds number and Schmidt number) only. It can be seen that even for small value of Schmidt number (large diffusion coefficient) the mixing is poor, as seen by the narrow spreading of concentration profile. The relatively larger diffusion at the walls is explained by the slower axial velocities in that region. It can be seen from Fig. 6a and b, that there is less mixing in the straight tube for  $Re = 0.1$  and  $Sc = 1000$  as compared to the  $Re = 100$  and  $Sc = 1$ . Fig. 6 also shows that, there is less mixing in the straight tube for  $Re = 0.1$  as compared to the  $Re = 20$  for the constant value of  $Sc = 1000$ . Vanka et al. (2004) have also observed similar behavior. Fig. 7 shows the variation of unmixedness coefficient ( $\theta$ ) as a function of distance ( $L/d$ ) along the tube for various values of Reynolds number and Schmidt number. Because the mixing is only attributed to diffusion and there are no

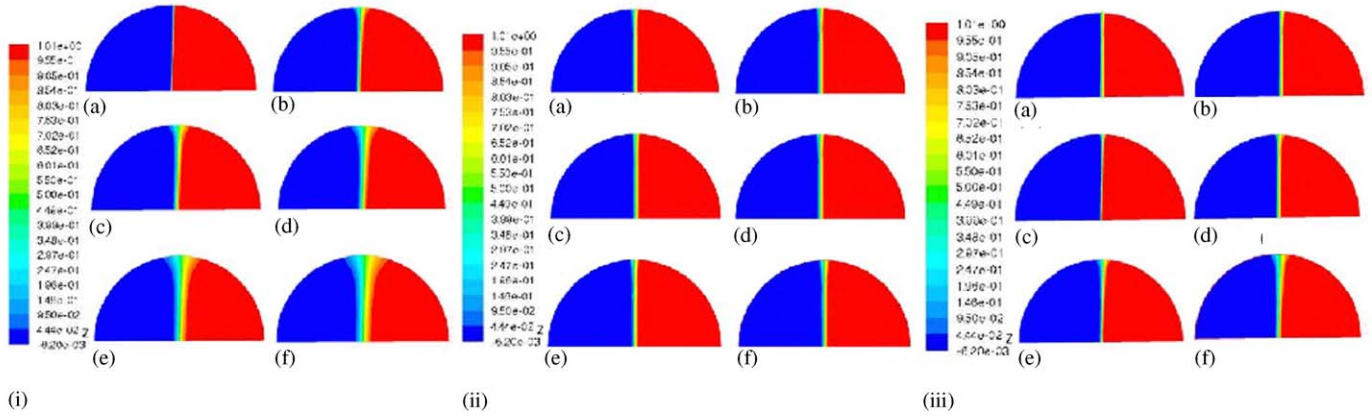


Fig. 6. Distribution of scalar concentration in a straight tube for: (i)  $Re = 100$  and  $Sc = 1$  ( $Re Sc = 100$ ); (ii)  $Re = 0.1$  and  $Sc = 1000$  ( $Re Sc = 100$ ); (iii)  $Re = 20$  and  $Sc = 1000$  ( $Re Sc = 20000$ ); and at (a)  $z = 0$ ; (b)  $z = 5$ ; (c)  $z = 10$ ; (d)  $z = 20$ ; (e)  $z = 40$  and (f)  $z = 60$ .

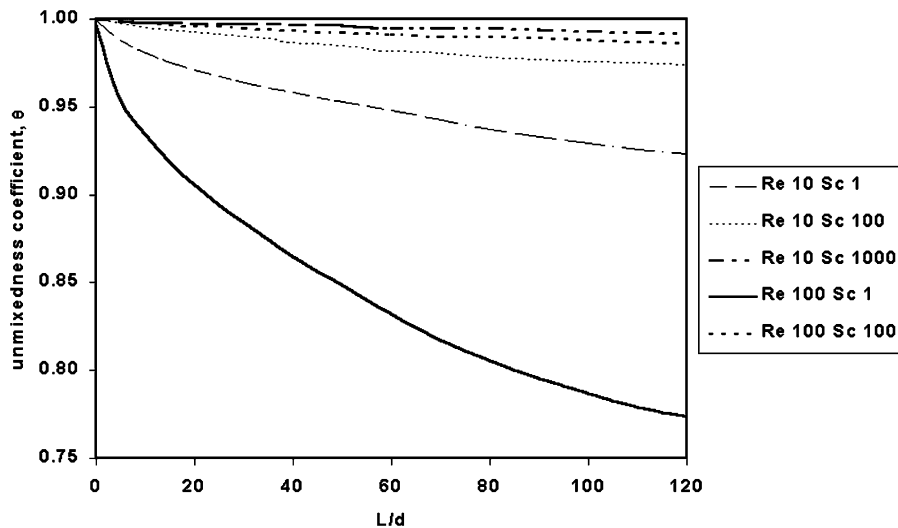


Fig. 7. Unmixedness coefficient as a function of distance along a straight tube.

cross-stream velocities present, the mixing is dependent on the scalar diffusivity only and it increases with decreasing  $Re Sc$  value.

### 3.2. Curved tube

In straight tube the mixing is governed by a single parameter ( $Re Sc$ ), while in a helical tube the mixing is more complex because of the secondary flow generation due to centrifugal forces that depend on the Reynolds number and the curvature ratio. Thus the mixing efficiency is a complex function of the Reynolds number, Schmidt number and curvature ratio of the tube. Therefore, the relative effectiveness of a helical tube is quite complicated and challenging over a straight tube because of centrifugal forces caused by curvature in the tube. Before proceeding to study the mixing in the curved tube of circular cross-section with finite pitch the velocity profiles at different

Dean numbers are presented as shown in Fig. 8 while Fig. 9 shows the velocity contours for coil of curvature ratio,  $\lambda = 10$ . It can be seen from the figures that as the Reynolds number increases the velocity profiles shift towards the outer wall of the curved tube. As the Reynolds number decreases the secondary flow also decreases in magnitude, being negligible for  $De = 0.32$ . Thus the effect of secondary flow is not significant for  $De = 0.32$ .

#### 3.2.1. Effect of Reynolds number

Fig. 10 shows the mixing behavior in curved tube through cross-sectional distributions of concentration after every  $180^\circ$  turn for different Reynolds numbers at given value of Schmidt number. At the inlet, the concentration is unity (red) in the inner half of the tube and zero (blue) in the outer half. Dean vortices are from the inner half to the outer half and the flow is symmetrical over the horizontal mid plane. It can be seen that

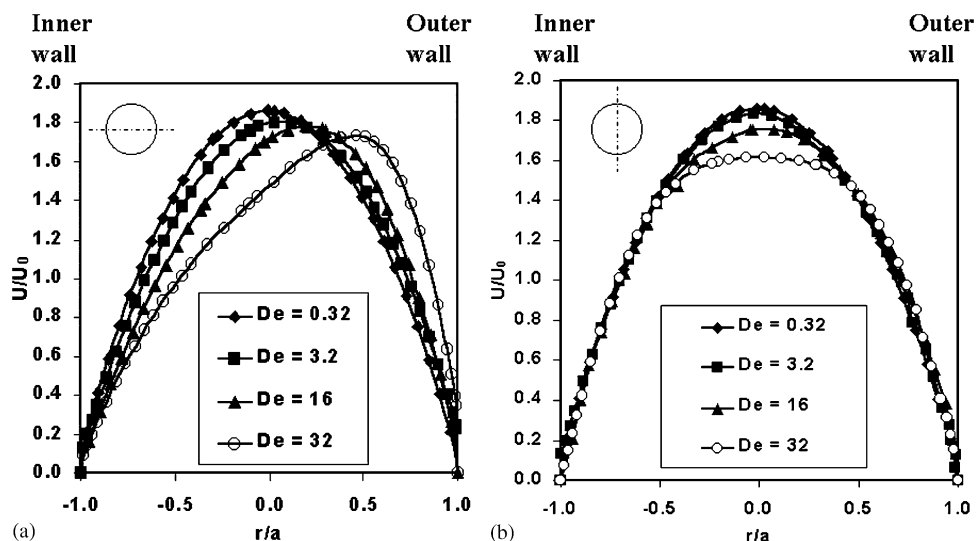


Fig. 8. Velocity profiles at different Dean numbers at  $\lambda = 10$  on (a) horizontal centerline and (b) vertical centerline.

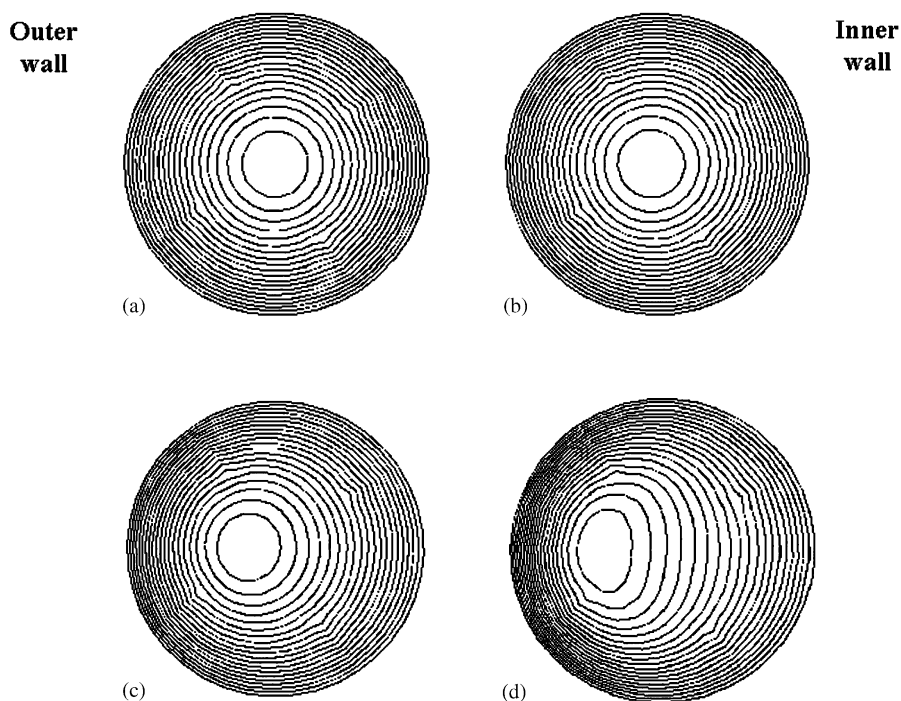


Fig. 9. Velocity fields at different Dean numbers at  $\lambda = 10$  on (a)  $De = 0.32$ , (b)  $De = 3.2$ , (c)  $De = 16.0$  and (d)  $De = 32.0$ .

the effect of Dean vortices is to bend the concentration contours and mix the two halves through advection of the concentration. However, at  $Re = 1.0$ , the Dean vortices are relatively weak and the mixing ascribed to secondary flow is not significant. When the Reynolds number is increased to 10, the mixing attributed to secondary flow is much stronger. On further increasing the value of Reynolds number to 20, the contours of concentration are much more deformed by the secondary flow, resulting

in enhanced surface area for diffusion and mixing. It can be observed that the distribution of concentration attained after 4 turns for  $Re = 10$  is obtained after only two turns for  $Re = 20$ . This also confirms the strong dependence of secondary flow on Reynolds number.

Fig. 11a summarizes the effect of Reynolds number on the mixing efficiency of curved tubes with flow length for different Schmidt number. It is observed that with increasing

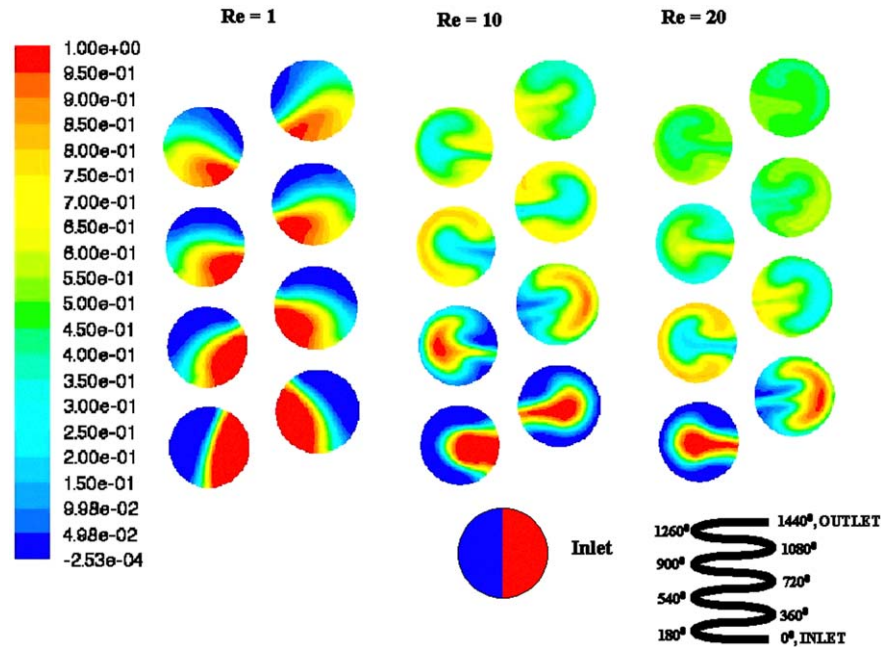


Fig. 10. Distribution of the scalar concentration in the helical tube ( $\lambda = 10$ ) for  $Sc = 1000$  after every  $180^\circ$  turn.

As  $Re$  increases the curves for different  $Sc$  values come closer and finally overlap each other for  $Re = 100$  (see Fig. 11f). This can be explained on the basis of relative magnitudes of the two mixing mechanisms operating simultaneously in the system due to the molecular diffusion and convection. As the Reynolds number increases the mixing due to secondary flow dominates over that due to molecular diffusion and the effect of  $Sc$  negligible. Fig. 11a shows the mixing efficiency for  $Re = 0.1$ , which is predominantly due to molecular diffusion therefore as the value of Schmidt number increases there is a significant effect on mixing efficiency. Further increase in the value of Reynolds number to 1 the molecular diffusion still dominates and there is no significant mixing. On further increasing the Reynolds number to 5 we can observe the shift in the pattern and the effect of Schmidt number is less pronounced for  $Sc$  values greater than 10 as shown in Fig. 11c (curves are closer). This is due to the secondary flow dominates over molecular diffusion at higher Reynolds number.

### 3.2.2. Effect of curvature ratio ( $\lambda$ )

To study the effect of curvature ratio on the mixing characteristics similar simulations were performed for a helical coil with  $\lambda = 5$ . Fig. 12 compares unmixedness coefficient for the two curvature ratios. It is observed that the curves are closer and lower for  $\lambda = 5$ ; this shows stronger mixing due to increased secondary flow. The intensity of secondary flow depends on the Dean number. For low value of Reynolds number ( $Re = 0.1$  and 1) there is no significant difference between the two curves while the difference is significant for higher values of Reynolds number ( $Re = 10$  and 100). This may be due to dominance of molecular diffusion mechanism at low Reynolds number, thus curvature ratio has insignificant effect on

mixing. For higher values of Reynolds number, mixing mechanism due to secondary flow is dominant thus mixing is better for  $\lambda = 5$ .

### 3.2.3. Mixing in coiled tube vs. straight tube

Fig. 13 shows the ratio of unmixedness coefficient in coiled tube ( $\theta_{\text{Coil}}$ ) of two different curvature ratios (i.e.,  $\lambda = 5$  and 10) to the straight tube ( $\theta_{\text{Straight}}$ ) for different values of Schmidt number varying from 1 to 1000 and constant value of Reynolds number ( $Re = 10$ ). It can be seen from the figure that, for the same values of  $Re Sc$  the mixing in coiled tube is higher as compared to straight tube. The mixing is reduced in the coiled tube as the curvature ratio increases, therefore coiled tubes of lower curvature ratio is preferable to achieve higher mixing.

## 4. Conclusion

In the present work a computational fluid dynamics study is performed in curved tubes of circular cross-section of finite pitch under laminar flow conditions to examine the scalar mixing of two miscible fluids using scalar transport technique. Two flow streams with inlet scalar concentrations of zero and unity in the two halves of a tube perpendicular to the plane of curvature was allowed to mix by convection and diffusion. It can be concluded that mixing in curved tubes at intermediate Reynolds number is far more efficient than a straight tube of similar dimensions. The mixing in curved tubes is significantly greater at higher Reynolds numbers, whereas in straight tubes, mixing efficiency decreases as the Reynolds number increases. In a curved tube, the increase in Reynolds number produces increased levels of secondary flow, which produce enhanced

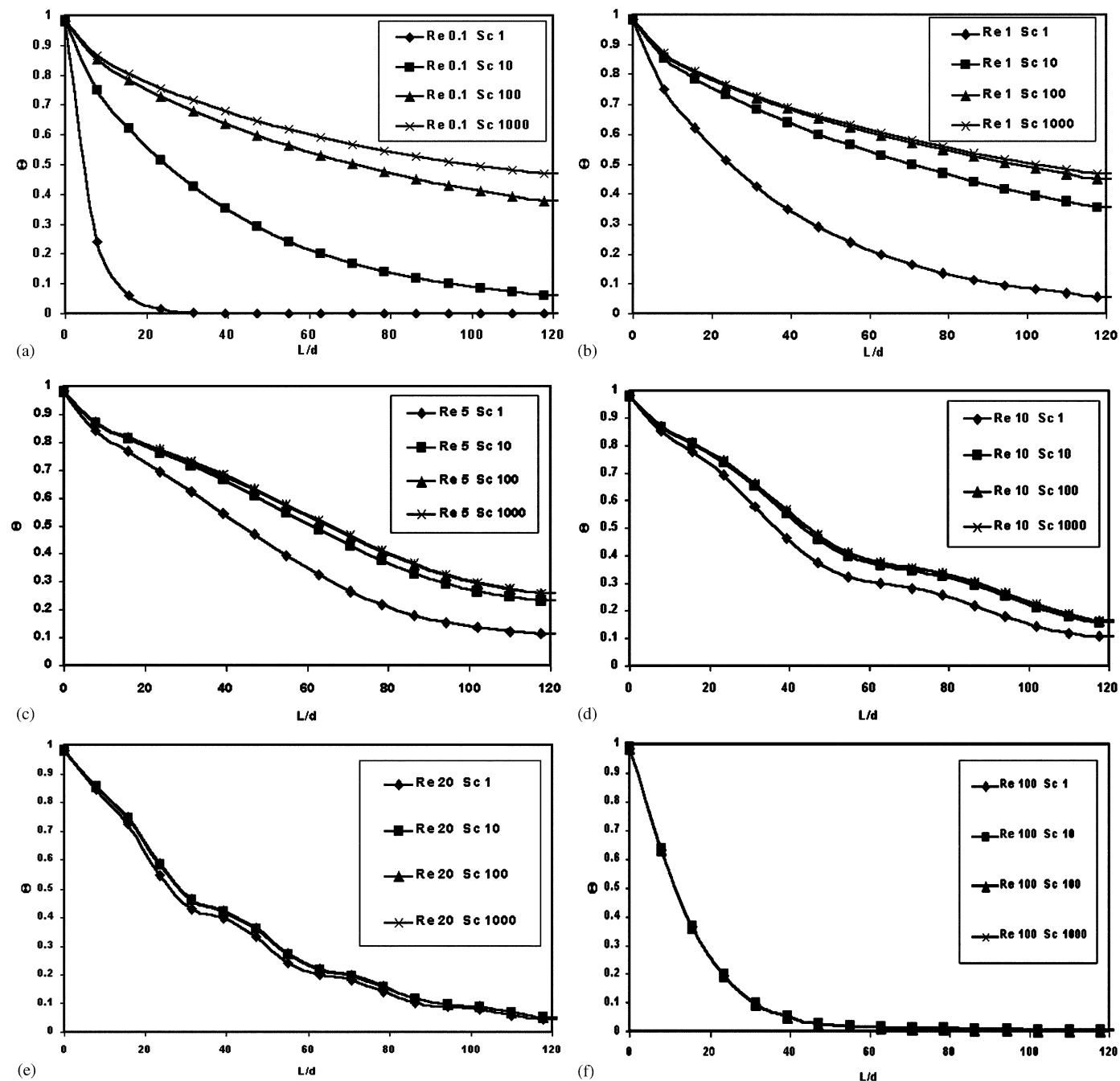


Fig. 11. Unmixedness coefficient as a function of distance along the curved tube ( $\lambda = 10$ ) for: (a)  $Re = 0.1$ ; (b)  $Re = 1$ ; (c)  $Re = 5$ ; (d)  $Re = 10$ ; (e)  $Re = 20$ ; and (f)  $Re = 100$ .

mixing. In contrast, the increase in Reynolds number in a straight channel decreases the residence time for diffusion to take place, and thus the mixing efficiency. Thus a balance of mixing mechanisms due to molecular diffusion and secondary flow exists in helical tubes. It was observed that at low Reynolds numbers, i.e., of the order of 0.1, curved tube mixers are not very attractive because of the low intensity of the secondary flow, but at higher values of Reynolds number, of the order of 10–100, curved tube present an efficient solution.

Especially in case of kenics-static mixers, there is decrease in mixing efficiency at higher Reynolds numbers due to the formation of dead zones (Muzzio and Hobbs, 1998; Muzzio and Szalai, 2003). Therefore curved tube mixers may provide an alternate solution for static mixers in the Reynolds number range of 10 to 100. It was also observed that at low curvature ratio (i.e.,  $\lambda = 5$ ) the secondary flows are stronger and mixing is higher as compared to the higher curvature ratio (i.e.,  $\lambda = 10$ ).

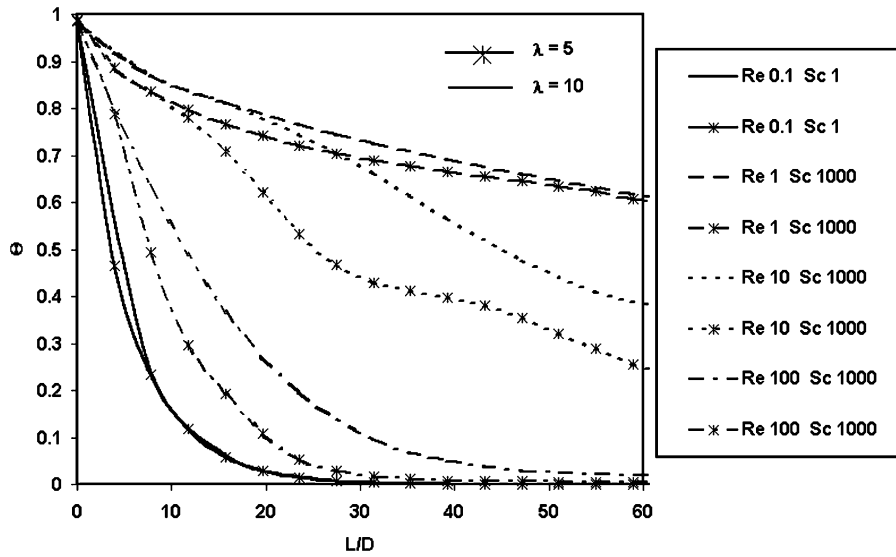


Fig. 12. Comparison of mixing curves for the two curvature ratios ( $\lambda = 5$  and 10).

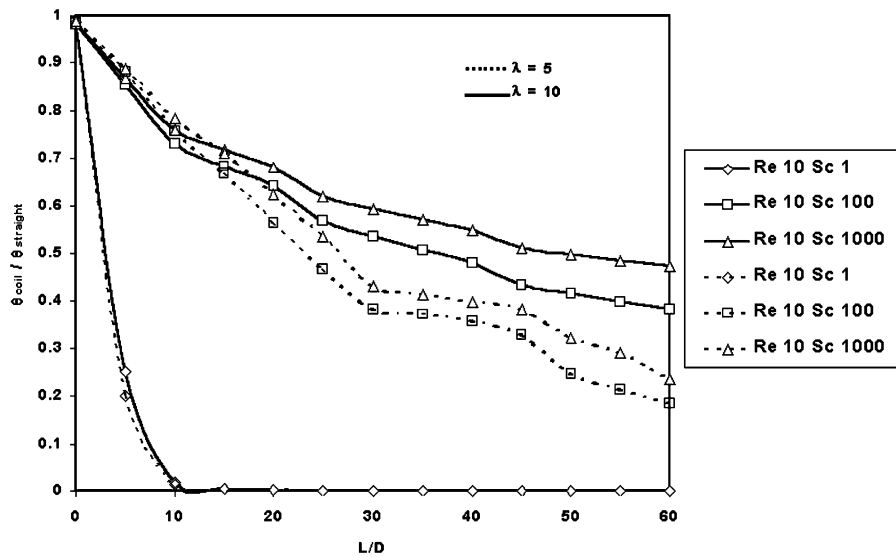


Fig. 13. Ratio of unmixedness coefficient in coiled tube ( $\lambda = 5$  and 10) to the straight tube ( $\theta_{Coil}/\theta_{Straight}$ ).

**Notation**

$a$	tube radius
$De$	Dean number ( $=Re/\sqrt{\lambda}$ )
$H$	pitch
$H'$	dimensionless pitch ( $=p/2\pi R_c$ )
$L$	tube length
$p$	pressure
$R_c$	coil radius
$Re$	Reynolds number ( $=dv\rho/\mu$ )
$Sc$	Schmidt number ( $=\mu/\rho\Gamma$ )
$u$	velocity component in the flow direction
$u_0$	inlet velocity
$x_i$	Cartesian coordinate in $i$ -direction [ $i = 1, 2$ and $3$ ]

$X, Y, Z$  master Cartesian coordinates  
 $z$  dimensionless tube length ( $=L/d$ )

*Greek letters*

$\Gamma$	diffusion coefficient
$\delta_{ij}$	direct delta function
$\theta$	unmixedness coefficient, roots mean square deviation of scalar from average value
$\lambda$	curvature ratio ( $D/d$ )
$\mu$	fluid viscosity
$\bar{v}$	fluid phase velocity
$\rho$	fluid density
$\tau$	shear stress tensor
$\phi$	scalar concentration

$\phi_{\text{avg}}$  flow weighted average of scalar concentration over a cross-section  
 $\varphi$  axial angle

### Subscript

0 inlet conditions

### References

- Bakker, A., LaRoche, R.D., Marshall, E.M., 1998. Laminar flow in static mixers with helical elements. The Online CFM book, at <http://www.bakker.org/cfm>.
- Berger, S.A., Talbot, L., Yao, L.S., 1983. Flow in curved pipes. *Annual Review of Fluid Mechanics* 15, 461.
- Bessoth, F.G., de Mello, A.J., Manz, A., 1999. Microstructure for efficient continuous flow mixing. *Analytical Communications* 36, 213–215.
- Boussinesq, J., 1891. Sur la maniere don't les vitesses, dans un tube cylindrique de section circulaire, evase a son entrée, se distribuent depuis entrée jusqu'aux endroits ou se trouve établi un regime uniforme. *Comptes Rendus* 113, 49–51.
- Branebjerg, J., Larsen, U.D., Blankenstein, G., 1996. Fast mixing by parallel multilayer lamination. In: *Proceedings of the Second International Symposium on Miniaturized Total Analysis Systems; Analytical Methods & Instrumentation, Special Issue  $\mu$ TAS'96*, Basel, pp. 228–230.
- Byrde, O., Sawley, M.L., 1999. Parallel computation and analysis of the flow in a static mixer. *Computers & Fluids* 28 (1), 1–18.
- Dean, W.R., 1927. Notes on the motion of fluid in a curved pipe. *Philosophical Magazine* 4, 208–233.
- Dean, W.R., 1928. The stream line motion of fluid in a curved pipe. *Philosophical Magazine* 5, 673–695.
- Deshmukh, A.A., Liepman, D., Pisano, A.P., 2000. Continuous micromixer with pulsatile micropumps. In: *Proceedings of Solid-State Sensor & Actuator Workshop*. Hilton Head, SC, June 4–8.
- Drese, K., 2003. Optimization of interdigital micromixers via analytical modeling—exemplified with the SuperFocus mixer. *Chemical Engineering Journal* 101 (1–3), 403–407.
- Duchene, Ch., Peerhossaini, H., Michard, P.J., 1995. On the velocity field and tracer patterns in a twisted duct flow. *Physics of Fluids* 7, 1307–1317.
- Durst, F., Ray, S., Unsal, B., Bayoumi, O.A., 2005. The development lengths of laminar pipe and channel flows. *Transactions of the ASME* 127, 1154–1160.
- Ehlers, St., Elgeti, K., Menzel, T., Wießmeier, G., 2000. Mixing in the offstream of a microchannel system. *Chemical Engineering and Processing* 39, 291–298.
- Ehrfeld, W., Golbig, K., Hessel, V., Lowe, H., Richter, T., 1999. Characterization of mixing in micromixers by a test reaction: single mixing units and mixer arrays. *Industrial and Engineering Chemistry Research* 38, 1075–1082.
- Evans, J., Liepmann, D., Pisano, A.P., 1997. Planar laminar mixer. In: *Proceedings of the IEEE Tenth Annual Workshop of MEMS Workshop*, Nagoya, Japan, pp. 96–101.
- Floyd, T.M., Losey, M.W., Firebaugh, S.L., Jensen, K.F., Schmidt, M.A., 2000. Novel liquid phase microreactors for safe production of hazardous speciality chemicals. In: Ehrfeld, W. (Ed.), *Microreaction Technology: Industrial Prospects*. Springer, Berlin, pp. 171–180.
- Fourcade, E., Wadley, R., Hoefsloot, C.J., Green, A., Iedema, P.D., 2001. CFD calculation of laminar striation thinning in static mixer reactors. *Chemical Engineering Science* 56 (23), 6729–6741.
- Glasgow, I., Aubry, N., 2003. Enhancement of microfluidic mixing using time pulsing. *Lab on a Chip* 3, 114–120.
- Hardt, S., Schönfeld, F., 2003. Laminar mixing in different interdigital micromixers—Part 2: numerical simulations. *A.I.Ch.E. Journal* 49 (3), 578–584.
- Hessel, V., Hardt, S., Löwe, H., Schönfeld, F., 2003. Laminar mixing in different interdigital micromixers—Part I: experimental characterization. *A.I.Ch.E. Journal* 49 (3), 566–577.
- Hong, C.-C., Choi, J.-W., Ahn, C.H., 2001. A novel in-plane passive micromixer using coanda effect. In: Ramsey, J.M., van den Berg, A. (Eds.), *Micro Total Analysis Systems*. Kluwer Academic Publishers, Dordrecht, pp. 31–33.
- Jen, C.-P., Wu, C.-Y., Lin, Y.-C., Wu, C.-Y., 2003. Design and simulation of the micromixer with chaotic advection in twisted microchannels. *Lab on a Chip* 3, 77–81.
- Jiang, F., Drese, K.S., Hardt, S., Küpper, M., Schönfeld, F., 2004. Helical flows and chaotic mixing in curved micro channels. *A.I.Ch.E. Journal* 50, 2297–2305.
- Jones, S.W., Thomas, O.M., Aref, H., 1989. Chaotic advection by laminar flow in twisted pipe. *Journal of Fluid Mechanics* 209, 335–357.
- Kumar, V., Nigam, K.D.P., 2005. Numerical simulation of steady flow fields in coiled flow inverter. *International Journal of Heat Mass Transfar* 48, 4811–4828.
- Lee, Y.-K., Deval, J., Tabeling, P., Ho, C.-M., 2001. Chaotic mixing in electrokinetically and pressure driven micro flows. In: *Microreaction Technology, IMRET 5: Proceedings of the Fifth International Conference on Microreaction Technology*. Springer, Berlin, pp. 185–191.
- Liu, R.H., Stremmer, M.A., Sharp, K.V., Olsen, M.G., Santiago, J.G., Adrian, R.J., Aref, H., Beebe, D.J., 2000. Passive mixing in a three-dimensional serpentine microchannel. *JMEMS* 9, 190.
- Liu, R.H., Ward, M., Bonanno, J., Ganser, D., Athavale, M., Grodzinski, P., 2001. Plastic in-line chaotic micromixer for biological applications. In: *Proceedings of the mTAS 2001 Symposium*. California, USA, pp. 163–164.
- Liu, R.H., Jianing, Y.J., Pindera, M.Z., Athavale, M., Grodzinski, P., 2002. Bubble-induced acoustic micromixing. *Lab on a Chip* 2, 151–157.
- Liu, R.H., Lenigk, R., Druyor-Sanchez, R.L., Yang, J., Grodzinski, P., 2003. Hybridization enhancement using cavitation microstreaming. *Analytical Chemistry* 75, 1911–1917.
- Löb, P., Drese, K.S., Hessel, V., Hardt, S., Hofmann, C., Löwe, H., Schenk, R., Schönfeld, F., Werner, B., 2004. Steering of liquid mixing speed in interdigital micromixers—from very fast to deliberately slow mixing. *Chemical Engineering and Technology* 27 (3), 340–345.
- Lu, L.-H., Ryu, K., Liu, C., 2001. A novel microstirrer and arrays for microfluidic mixing. *Fifth International Conference on Miniaturized Chemical and Biochemical Analysis Systems*, October 21–25, 2001.
- Miyake, R., Lammerink, T.S.J., Elwenspoek, N., Fluitman, J.H.J., 1993. Micromixer with fast diffusion. In: *IEEEMEMS' 93*. Fort Lauderdale, USA, pp. 248–253.
- Mori, Y., Nakayama, W., 1965. Study on forced convective heat transfer in curved pipes. *International Journal of Heat Mass Transfer* 8, 67–82.
- Muzzio, F.J., Hobbs, D.M., 1998. Reynolds number effects on laminar mixing in the Kenics static mixer. *Chemical Engineering Journal* 70, 93–104.
- Muzzio, F.J., Szalai, E.S., 2003. Fundamental approach to the design and optimization of static mixers. *A.I.Ch.E. Journal* 49, 2687–2699.
- Nandakumar, K., Masliyah, J.H., 1986. Swirling flow and heat transfer in coiled and twisted pipes. In: Mujumdar, A.S., Masliyah, R.A. (Eds.), *Advances in Transport Process*, vol. 4. Wiley, Eastern, New York.
- Niu, X., Lee, Y., 2003. Efficient spatial-temporal chaotic mixing in microchannels. *Journal of Micromechanics and Microengineering* 13, 454.
- Oddy, M.H., Santiago, J.G., Mikkelsen, J.C., 2001. Electrokinetic instability micromixing. *Analytical Chemistry* 73 (24), 5822–5832.
- Palk, P., Pamula, V.K., Fair, R.B., 2003. Rapid droplet mixers for digital microfluidic systems. *Lab on a Chip* 3, 253–259.
- Patankar, S.V., Pratap, V.S., Spalding, D.B., 1974. Prediction of laminar flow and heat transfer in helically coiled pipes. *Journal of Fluid Mechanics* 62, 539–551.
- Penth, B., 1999. Method and device for carrying out chemical and physical processes, WO 00/61275. Germany.
- Qian, S., Bau, H.H., 2002. A chaotic electro-osmotic stirrer. *Analytical Chemistry* 74, 3616–3625.
- Saxena, A.K., Nigam, K.D.P., 1984. Coiled configuration for flow inversion and its effect on residence time distribution. *A.I.Ch.E. Journal* 30, 363–368.
- Schönfeld, F., Hardt, S., 2003. Simulation of helical flows in microchannels. *A.I.Ch.E. Journal* 50, 2297–2305.

- Schönfeld, F., Hessel, V., Hofmann, C., 2004. An optimised split-and-recombine micro mixer with uniform chaotic mixing. *Lab on a Chip* 4, 65–69.
- Schwesinger, N., Frank, T., Wurmus, H., 1996. A modular microfluidic system with an integrated micromixer. *Journal of Micromechanics and Microengineering* 6, 99–102.
- Shah, R.K., Joshi, S. K., 1987. Convective heat transfer in curved ducts. In: *Handbook of Single-Phase Convective Heat Transfer*, pp. 5.3–5.47 and 3.1–3.147.
- Solomon, T.N., Mezic, I., 2003. Uniform resonant chaotic mixing in fluid flows. *Nature* 425, 376–380.
- Stroock, A.D., Dertinger, S.K.W., Ajdari, A., Mezic, I., Stone, H.A., Whitesides, G.M., 2002a. Chaotic mixer for microchannels. *Science* 295, 647.
- Stroock, A.D., Dertinger, S.K.W., Ajdari, A., Mezic, I., Stone, H.A., Whitesides, G.M., 2002b. Patterning flows using grooved surfaces. *Analytical Chemistry* 74 (20), 5306–5312.
- Vanka, S.P., Luo, G., Winkler, C.M., 2004. Numerical study of scalar mixing in curved channels at low reynolds numbers. *A.I.Ch.E. Journal* 50, 2359–2368.
- Voldman, J., Gray, M.L., Schmidt, M.A., 1998. Liquid mixing studies with an integrated mixer/valve. In: Harrison, J., van den Berg, A. (Eds.), *Micro Total Analysis Systems*. Kluwer Academic Publishers, Dordrecht, pp. 181–184.
- Volpert, M., Meinhardt, C.D., Mezic, I., Dahleh, M., 1999. An actively controlled micromixer. In: *Proceedings of MEMS, ASME, IMECE Conference*, Nashville, TN, pp. 483–487.
- Werner, B., Koch, M., Wehle, D., Scherer, S., Forstinger, K., Meudt, A., Hessel, V., Loewe, H., 2002. Specially suited micromixers for process involving strong fouling. In: *Sixth International Conference on Microreaction Technology*, IMRET 6, New Orleans, USA. A.I.Ch.E. Publications No. 164, pp. 168–183.
- West, J., Boris Karamata, B., Lillis, B., Gleeson, J.P., Alderman, J., Collins, J.K., Lane, W., Mathewson, A., Berney, H., 2002. Application of magnetohydrodynamic actuation to continuous flow chemistry. *Lab on a Chip* 2, 224–230.
- Wojas, P., Hauser, K., Yacoub-George, E., 2000. An active silicon micromixer for  $\mu$ TAS applications. In: van den Berg, A., Olthuis, W., Bergveld, P. (Eds.), *Micro Total Analysis Systems*. Kluwer Academic Publishers, Dordrecht, pp. 277–282.
- Yang, Z., Matsumoto, S., Goto, H., Matsumoto, M., Maeda, R., 2001. Ultrasonic micromixer formicrofluidic systems. *Sensors and Actuators A* 93, 266–272.
- Yi, M., Bau, H.H., 2000. The kinematics of bend-induced stirring by micro-conduits. *Proceedings of MEMS, ASME, IMECE Conference*, vol. 2, pp. 489–496.
- Zech, T., Hönicke, D., Fichtner, M., Schubert, K., 2000. Superior performance of static micromixers. In: *Fourth International Conference on Microreaction Technology*, IMRET 4, Atlanta, USA. A.I.Ch.E. Topical Conference Proceedings, pp. 390–399.

### Further reading

- Paul, E.L. Paul, V.A.-O., Suzanne, M. *Handbook of Industrial Mixing: Science and Practice*. Wiley/IEEE, New York, pp. 873–876.
- Werner, B., Hessel, V., Löb, P., 2005. Mixers with microstructural foils for chemical production purposes. *Chemical Engineering and Technology* 28, 4.